Letter of Intent for J-PARC 30-GeV Proton Synchrotron:

Investigating $\bar{d}$+^{12}C nucleus interaction at J-PARC

T. Akaishi[1], C. Curceanu[14], C. Han[7], T. Hashimoto[3], T. Isobe[3], K. Itahashi[3], M. Iwasaki[3], S. Kanda[6], D.X. Lin[7], Y. Ma[3], R. Murayama[3], M. Niiyama[11], H. Noumi[1], H. Ohnishi[4], S. Okada[13], F. Sakuma[3], M. Sasano[3], B. Scavino[9], A. Scordo[14], R. Sekiya[16], K. Shirotori[1], F. Sirghi[14], D. Suzuki[3], K. Suzuki[1], T. N. Takahashi[1], U. Tamponi[8], M. Tanaka[12], K. Tanida[5], K. Tsukada[15], M. Ukai[6], H. Wang[3] T. Yamaga[6] T. O. Yamamoto[2], X. Yuan[7], Y. Zhang[7], H. Zhang[10]

[1]Osaka University, Osaka, 560-0043, Japan
[2]Japan Atomic Energy Agency, Ibaraki 319-1195, Japan
[3]RIKEN, Wako, 351-0198, Japan
[4]Tohoku University, Miyagi, 982-0826, Japan
[5]Japan Atomic Energy Agency, Tokai, 319-1195, Japan
[6]KEK, Tsukuba, 305-0801, Japan
[7]Institute of Modern Physics, Chinese Academy of Sciences, Lanzhou, 730000, China
[8]INFN Sezione di Torino, Turin, Italy
[9]Department of Physics and Astronomy, Uppsala University, Sweeden
[10]School of Nuclear Science and Technology, Lanzhou University, Lanzhou, 730000, China
[11]Department of Physics, Kyoto Sangyo University, Kyoto, 603-8555, Japan
[12]Faculty of Science and Engineering, Waseda University, Tokyo, 169-8555, Japan
[13]College of Science and Engineering, Chubu University, Kasugai, 487-8501, Japan
[14]Laboratori Nazionali di Frascati dell' INFN, I-00044 Frascati, Italy
[15]Institute for Chemical Research, Kyoto University, Kyoto, 611-0011, Japan
[16]Department of Physics, Kyoto University, Kyoto, 611-0011, Japan

Executive Summary

As the first step toward understanding antimatter composed of multiple antinucleons, we propose to investigate the antideuteron and its interactions with nucleus using $\bar{d}$ beam at the K1.8 beam line of the J-PARC Hadron Facility.
The proposed experiment will use the $\bar{d}$+^{12}C reaction to study the multiple $\bar{N}-N$ interactions. There are two main objectives for this experiment: measure the total and partial absorption cross section to derive the optical potential between $\bar{d}$ and ^{12}C nucleus; study multiple $\bar{N}-N$ annihilation mechanism by measuring annihilation phase space via $\pi^{\pm}$ momentum.
The major parameters of this experiment are summarized below:

	Beam line	:	K1.8
Commissioning	Purpose	:	Optimize $\bar{d}$ yield
	Secondary beam	:	1.8 GeV/c $\bar{d}$
	Main apparatus	:	K1.8 beam line
	Beam time	:	80 kW $\times$ 2 days
Physics run	Purpose	:	Derive $\bar{d}$–^{12}C optical potential and study multiple $\bar{N}-N$ annihilation mechanism
	Secondary beam	:	1.8 GeV/c $\bar{d}$
	Reaction	:	$\bar{d}$+^{12}C
	Main apparatus	:	KURAMA dipole spectrometer
	Beam time	:	1×10^6 $\bar{d}$ beam particles

Contents

1 Introduction

Antimatter has held a significant position within both the scientific community and popular culture for many years. It has captured attention ranging from testing CPT violation [1, 2] to its portrayal in Hollywood movies [3], symbolizing humanity's unrelenting pursuit of the unknown. The investigation into antimatter and its dynamic interplay with matter remains intricately intertwined with one of contemporary physics' most profound enigmas: the antimatter-matter imbalance. Numerous investigations into antiprotons ($\bar{p}$) and their interaction with matter have been undertaken to address this puzzle [4].

However, the exploration of antinuclei composed of multiple antinucleons, such as the antideuteron ($\bar{d}$), remains relatively unexplored territory. For instance, only absorption cross sections on heavy targets are reported at 13.3 GeV/c and 25 GeV/c without information about their reaction products as shown in Fig. 1 [5, 6]. A recent study by the ALICE collaboration shown in Fig. 2 provides the total inelastic cross section between $\bar{d}$ and the averaged detector materials ($< A >= 17.4$ and $< A >= 31.8$) as effective targets, without details about the reactions [7].

As a foundational step toward understanding antimatter composed of multiple antinucleons, we propose to investigate the antideuteron using a $\bar{d}$ beam at the K1.8 beam line of the J-PARC Hadron Facility. In this proposal, we aim to address the following topics:

1. How does $\bar{d}$ interact with nucleus? By adding one more antinucleon, how will the $\bar{d}-$nucleus potential differ from $\bar{p}-$nucleus?

2. How will the antinucleus annihilate with nucleus? Will the two antinucleons inside $\bar{d}$ annihilate with nucleons from nucleus independently or simultaneously?

The proposed experiment will be conducted at the K1.8 beam line of the J-PARC Hadron Facility. The $\bar{d}$ beam momentum is set to 1.8 GeV/c in order to maximize the sensitivity of the $\bar{d}-$nucleus optical potential [9]. A 10 cm thick ^{12}C graphite target will be used to enhance luminosity. A dipole magnet spectrometer, KURAMA, will detect the reaction products. The detailed experimental setup and the physics motivation are described in the following sections.

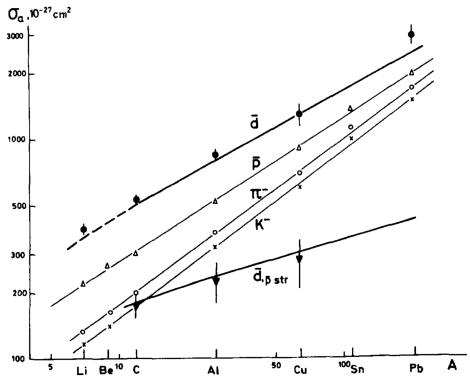

(a) $\bar{d}$ absorption cross section with various targets at 13.3 GeV/c [5].

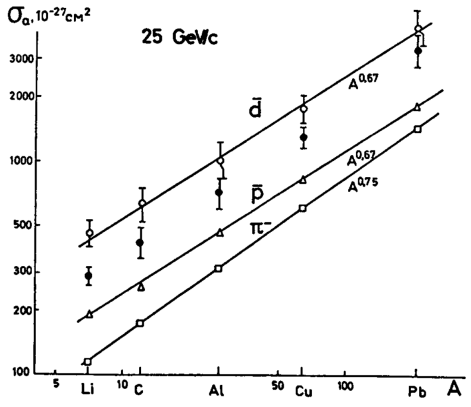

(b) $\bar{d}$ absorption cross section with various targets at 25 GeV/c [6].

Figure 1: $\bar{d}$ absorption cross section measured in 1970s at JINR.

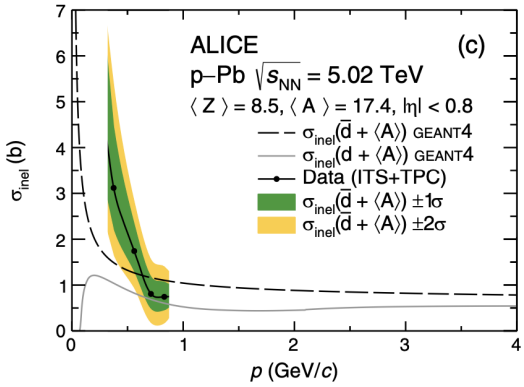

(a) $\bar{d}$ inelastic cross section with P $<$ 1.0 GeV/c.

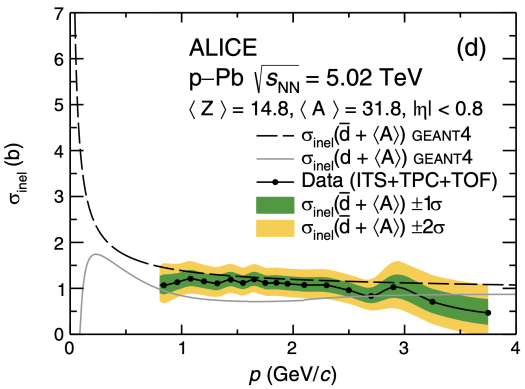

(b) $\bar{d}$ inelastic cross section with P $>$ 1.0 GeV/c.

Figure 2: Inelastic cross section of $\bar{d}$ on ALICE detector as effective target [7].

2 Physics motivation

In this section, we will discuss the physics motivation behind the proposed experiment. The main topics to be addressed are the $\bar{d}-$nucleus optical potential and the multiple $\bar{N} - N$ annihilation mechanism. The effectiveness of the proposed method will be demonstrated through calculations using the GiBUU package [23].

2.1 Study $\bar{d}-$nucleus optical potential

The interaction between antimatter and matter has been a topic of fundamental importance since the discovery of the antiproton in 1955 [8]. Within the framework of Relativistic Mean Field Theory (RMF), the $\bar{p}-$nucleus interaction is expected to be extraordinarily strong due to the flip of G-parity. This flip results in both the scalar and vector potentials becoming attractive, a situation that is usually canceled out in the case of nucleons. A calculation performed exploiting the G-parity flipping returns a potential of of $V \sim -600$ MeV [9].

However, experimental results from both $\bar{p}$-atomic X-ray measurements [10, 11] and $\bar{p}-$nucleus elastic scattering experiments [12] suggest a much weaker interaction, with $V \sim -100$ MeV. One possible explanation for this discrepancy is the large probe distance in both approaches, which makes them sensitive only to the long-range part of the potential. In contrast, the $\bar{p}$ absorption cross section is expected to be more sensitive to the short-range part by penetrating into the nuclear medium and causing absorption. For instance, $\bar{p}$ at 0.6 GeV/c can reach an average of 50% nuclear density before absorption occurs. In this case, the potential is derived as $V \sim -150$ MeV [9].

Another important factor contributing to the deviation from the RMF prediction is the short lifetime of the $\bar{p}-$nucleus system. Regardless of the experimental approach mentioned above, the virtual potential obtained so far consistently shows $W \geq 100$ MeV. Such a strong virtual potential (i.e. the short lifetime) makes it difficult for the $\bar{p}$ nucleus state to reach an equilibrium state before annihilation, which is required by the RMF prediction.

While we have some understanding of the $\bar{p}-$nucleus interaction, the $\bar{d}-$n interaction remains an open question. The $\bar{d}$ nucleus is composed of two antinucleons, making it a unique system for studying multiple $\bar{N} - N$ interactions. If we assume the $\bar{d}-$nucleus system has a similar lifetime to that of the $\bar{p}-$nucleus system, a linear extrapolation from the $\bar{p}-$nucleus potential gives $V - 200 \sim -300$ MeV due to the presence of two attractive centers. This raises the question: Will such a strong attractive potential modify the nucleus structure and the lifetime of the $\bar{d}-$nucleus system? This is one of the key questions we aim to address in this proposal.

In order to investigate quantitatively the $\bar{d}-$nucleus interaction, we will utilize GiBUU, a transport model-based calculation package developed by Giessen University, Germany [23]. GiBUU has been

widely used to study $\bar{p}-$nucleus interactions, showing impressive agreement with experimental data [9]. Thanks to the kind support of Dr. K. Gallmeister of the GiBUU group, a $\bar{d}$ beam is now available in the GiBUU package.

To motivate and support our proposal, we performed calculations for the $\bar{d}+^{12}$C reaction with different strengths for the real part of the optical potential. We found that the ratio between partial (σ_{ParAnn}) and coherent (σ_{CohAnn}) annihilation cross sections is very sensitive to the strength of the optical potential. Here, partial annihilation refers to the reaction where only one antinucleon from $\bar{d}$ annihilates with a target nucleon, while coherent annihilation refers to the reaction where both antinucleons from $\bar{d}$ annihilate with target nucleons.

More specifically, for a $\bar{d}$ beam at 1.8 GeV/c, if we assume $V = -150$ MeV between $\bar{N}-$nucleus as derived from $\bar{p}-$nucleus absorption experiment data, the ratio $\sigma_{ParAnn}/\sigma_{CohAnn}$ is approximately 2.8. If we set $V = -300$ MeV between $\bar{N}-$nucleus, the ratio $\sigma_{ParAnn}/\sigma_{CohAnn}$ becomes 1.6, indicating a sensitive dependence. This observation suggests that the ratio between these two cross sections can be used to derive the strength the $\bar{d}-$nucleus optical potential.

From an intuitive perspective, the sensitivity of the ratio $\sigma_{ParAnn}/\sigma_{CohAnn}$ regarding the $\bar{d}-$nucleus optical potential becomes apparent when considering the attractive force between the $\bar{d}$ and the nucleus. A stronger force draws the antinucleons nearer to the nucleus, consequently increasing the likelihood of coherent annihilation. [1]

2.2 Investigate multiple $\bar{N}-N$ annihilation mechanism

Another interesting topic will be addressed in this experiment: the multiple $\bar{N}-N$ annihilation mechanism. In order to facilitate the discussion, we classify the $\bar{d}+^{12}$C coherent annihilation into the following three scenarios:

1. Two-Step Independent Annihilation: This involves two independent $\bar{N}-N$ pairs, each annihilating without affecting the other, akin to having two separate $\bar{p}-p$ annihilation.

2. Correlated Cascade Annihilation: In this scenario, one of the mesons produced from the first $\bar{N}-N$ annihilation is absorbed by the second pair before their reaction. The sequence of reactions is: $\bar{N}+N \to (n-1)\pi$, $\pi+\bar{N} \to \bar{\Delta}$ (or $\pi+N \to \Delta$), and $\bar{\Delta}+N \to n\pi$ (or $\Delta+\bar{N} \to n\pi$). Consequently, the second annihilating pair will have a larger phase space available for annihilation reaction due to the increase in total energy.

3. One-Step Simultaneous Annihilation: If both $\bar{d}$ and ^{12}C are in a short-range correlated (SRC) state during $\bar{d}-2N$ annihilation, the annihilation phase space can expand up to 4 GeV. This extreme case will produce pions with high momentum beyond the kinematic limits of the other two scenarios.

At first glance, all three scenarios produce high-multiplicity final states, making it challenging to distinguish them experimentally. However, the well studied $\bar{p}-p$ annihilation can provide valuable insights. As shown in Figs. 3 and 4, multiple $\pi^{\pm,0}$ final states dominate $\bar{p}-p$ annihilation at rest [22]. A Gaussian fit to the multiplicity distribution in Fig. 3 yields a mean multiplicity of 5.01 and a standard deviation of $\sigma = 1.04$. The $\pi^{\pm,0}$ momentum distribution in Fig. 4 closely resembles a pure phase space distribution, suggesting that $\bar{p}-p$ annihilation can be understood as a reconfiguration of $\bar{q}-q$ pairs with equal probability.

This observation suggests that the π momentum distribution can be exploit to distinguish experimentally between the three annihilation scenarios in the $\bar{d}+^{12}$C system. Specifically, the total phase space is dictated by the initial total energy, and the multiplicity is directly proportional to the energy available for the annihilation reaction. Drawing from the insights gained from $\bar{p}-p$ annihilation studies,

[1] One should note that if the so obtained potential between $\bar{d}$ and nucleus is not so extraordinarily strong that the distortion for the $\bar{d}$ and nucleus wave function are negligible, the $\bar{d}+^{12}$C coherent annihilation cross section can be used to derive the $\bar{d}$ radius for the first time, which is a key to allow us to test the nuclear force universality.

where the multiplicity of the final state $\pi^{\pm,0}$s is crucial, we hypothesize that the π multiplicity correlates with the total energy of the annihilation partners.

For the One-step Simultaneous Annihilation, we propose the following relations:

$$\begin{aligned} \text{multiplicity} &= \frac{\text{total energy of } \bar{d}+2N}{\text{mass of } \bar{p}+p} \times 5.01 \\ \sigma &= \frac{\text{total energy of } \bar{d}+2N}{\text{mass of } \bar{p}+p} \times 1.04, \end{aligned} \tag{1}$$

where 5.01 and 1.04 are the mean and standard deviation of π multiplicity from $\bar{p}-p$ annihilation at rest, respectively. Similarly, for a correlated cascade annihilation, we can determine the total energy of the $\bar{\Delta}+N$ (or $\Delta+\bar{N}$) system by combining a random pion from the first annihilation with the second $\bar{N}-N$ pair. The resulting π momentum distribution is depicted in Fig. 5, 6, and 7.

For the two-step independent annihilation, characterized by a phase space of approximately 2.24 GeV for a $\bar{p}$ beam at 0.9 GeV/c, the π momentum distribution extends up to ~ 1.6 GeV/c. In contrast, the one-step simultaneous annihilation yields a phase space roughly twice as large as the independent case, amounting to approximately 4.5 GeV. Consequently, the resulting π momentum distribution exhibits a much broader spread, extending beyond the kinematic limit observed in the $\bar{p}-p$ case. In the case of correlated cascade annihilation, the π momentum distribution falls between the ranges observed in these two extreme scenarios. [2]

To further validate the proposed method, we calculated the $\bar{d}$+^{12}C reaction using the GiBUU package with default parameters optimized for the $\bar{p}$ data. The calculated π momentum distribution is shown in Fig. 8 and 9. The slight excess of π momentum than 1.6 GeV/c in partial annihilation visible in Fig. 8 is due to the Fermi motion contribution, which is about $\sim 10\%$ of the signal events given in Fig. 9. Fig. 9 shows the highest number of events above the kinematic limit as a result of the Correlated Cascade Annihilation from GiBUU. [3] The results are consistent with our phase space based estimation, indicating that the π momentum distribution can be used to distinguish between the three annihilation scenarios. [4]

Before concluding this section, we would like to point out that the proposed measurement for the One-Step Simultaneous Annihilation provides a unique opportunity to study the short-range correlated (SRC) state in both $\bar{d}$ and ^{12}C nucleus in spatial distribution. The SRC state is an important topic which might be related to the EMC effect. However, the study of the SRC so far has been limited to the momentum space: what has been observed in the electron scattering data is the back-to-back correlation of high-momentum nucleons [13]. One has to rely on the uncertainty principle to infer the spatial distribution from the momentum distribution. In our proposed experiment, the One-Step Simultaneous Annihilation, if observed, can only come from very tight spatial overlap of the $\bar{d}$+^{12}C wave functions. Therefore, we will have the first chance to verify the SRC state in spatial distribution.

[2] Qualitatively, the rationale for utilizing the π momentum distribution to distinguish between the three scenarios is as follows: the kinematic constraints governing the π momentum distribution are directly linked to the annihilation phase space, which scales with the total energy of the annihilation partners.

[3] One should note that, however, the One-Step Simultaneous Annihilation is not included in the GiBUU calculation.

[4] The statistics and significance for the proposed method will be covered in the Section3.2.

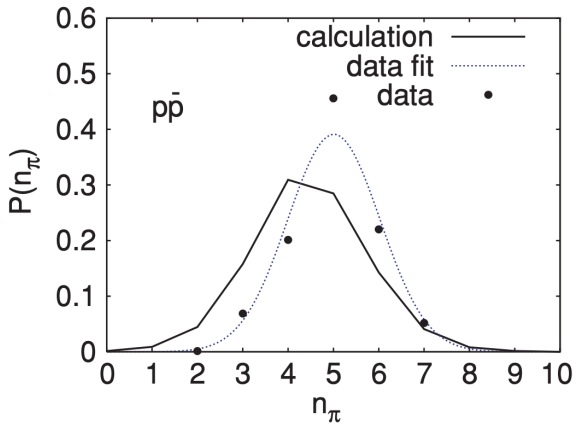

Figure 3: π multiplicity from $\bar{p}-p$ annihilation at rest.

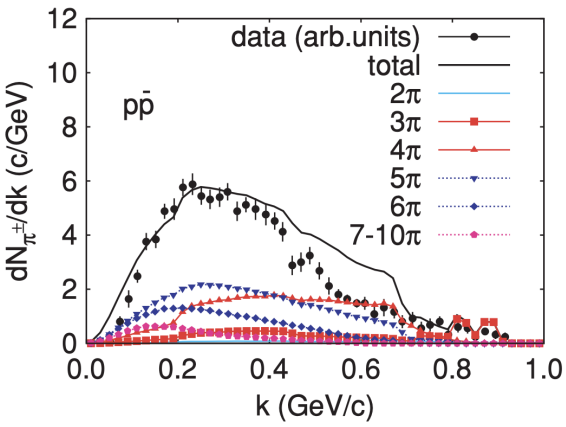

Figure 4: π momentum distribution from $\bar{p}-p$ annihilation at rest.

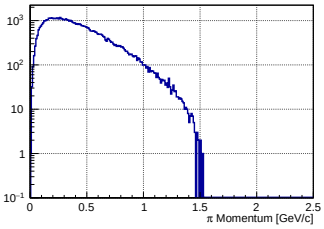

Figure 5: π momentum distribution from Two-Step Independent Annihilation.

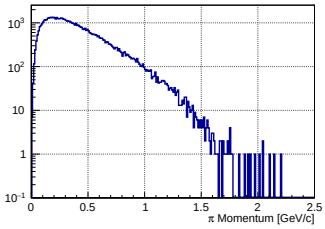

Figure 6: π momentum distribution from Correlated Cascade Annihilation.

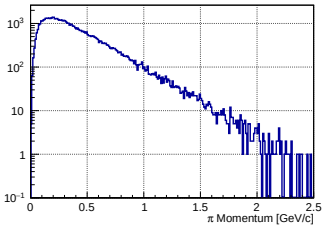

Figure 7: π momentum distribution from One-Step Simultaneous Annihilation.

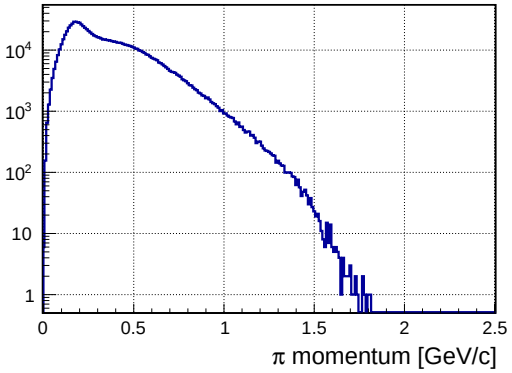

Figure 8: π momentum distribution from $\bar{d}$+^{12}C partial annihilation events.

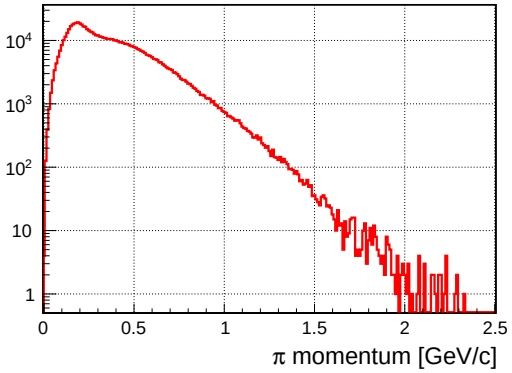

Figure 9: π momentum distribution from $\bar{d}$+^{12}C coherent annihilation events.

3 Experimental setup and performance estimation

This section describes the experimental setup for the proposed $\bar{d}$+^{12}C reaction experiment. The setup consists of a dipole type spectrometer with KURAMA magnet, a graphite target and tracking detectors. The thickness of the graphite target is determined by GiBUU to be 10 cm, in order to fully react with the $\bar{d}$ beam particles. With the proposed 1×10^6 $\bar{d}$ beam particles on the graphite target, we can expect 1.3×10^5 coherent annihilation and 4.0×10^5 partial annihilation reaction events, respectively.

3.1 $\bar{d}$ beam intensity at K1.8 beam line

In a pre-study conducted by one of the authors, M. Ukai, the existence of antideuteron beam has been confirmed. As shown in Fig. 10, the antideuteron can be identified by its Time-of-Flight (TOF). Within a very limited time slot for this pre-study, $\bar{d}$ particles were identified with 326 spills at 64 kW beam power. As described in Ref. [14], ~ 0.3 $\bar{d}$/spill (~ 5 seconds) is obtained, which will be used through out this proposal for yield estimation.

It should be noted that the beam line configurations were not optimized for the $\bar{d}$ beam at that time. If we scale the $\bar{d}$ yield based on the $\bar{p}$ intensity, we can expect at least ~ 3 times higher $\bar{d}$ beam intensity by fully optimizing the beam line setup, which will be carried during commissioning phase of this proposal. With this $\bar{d}$ beam intensity, we can accumulate the proposed 1×10^6 $\bar{d}$ beam with ~ 2 months of beam time.

We would also like to point out that the production mechanism of $\bar{d}$ at energies below 2.0 GeV/c using high energy protons is still largely unknown [15]. A detailed scan of the $\bar{d}$ yield, along with beam transportation calculations for the K1.8 beam line, could provide some insight into this topic and help us to test the coalescence model.

Another interesting direction waiting to be explored is that according to Ref. [16], the antideuteron yield will be approximately an order of magnitude higher at 6.0 GeV/c. However, as the first experiment to investigate antimatter-matter interactions, we will focus on the $\bar{d}$ physics with relatively low momentum and leave this possibility for future exploration.

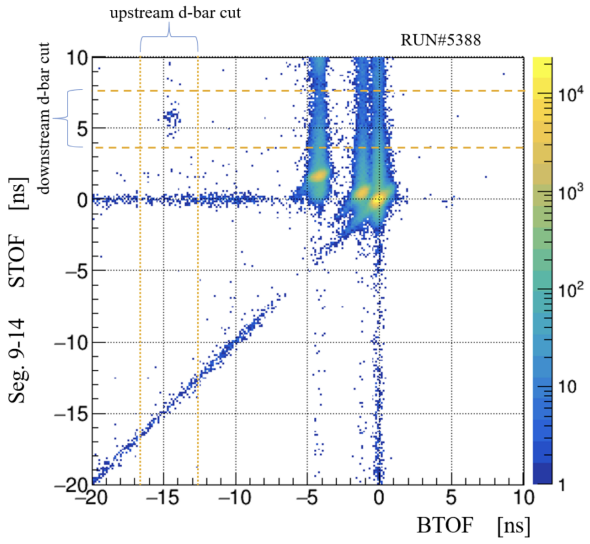

Figure 10: K1.8 beam line TOF vs downstream TFO spectrum, from which the $\bar{d}$ particles are clearly identified.

3.2 Experimental setup

To fully utilize the antideuteron beam with very low intensity as described in Section 3.1, we propose an experimental setup as shown in Fig. 11. This setup includes 10 thin slices of graphite target with a total thickness of 10 cm. The total thickness of graphite is so chosen that the $\bar{d}$ beam particles can fully react with ^{12}C target nucleus. Each slice of the graphite target has a thickness of 10 mm to minimize the probability of successive partial annihilation, which can fake a coherent annihilation and contributes as major systematic uncertainty in the derivation of the σ_{ParAnn} and σ_{CohAnn}, as will be described in section 3.3.

The central component of the dipole spectrometer is the KURAMA magnet, which is characterized by a large acceptance and a high magnetic field of 0.78 T. The KURAMA magnet has a gap of 80 cm in height, 100 cm in width and 80 cm in length. Four sets of drift chambers are installed inside the KURAMA magnet to track the charged particles originating from the annihilation reaction. The drift chambers are also placed upstream of the target to cover the backward region for acceptance of the reaction products. A barrel scintillation fiber tracker surrounds the target to catch reaction products in the central angular region. Finally, a forward scintillation counter wall (FwdTOF) is placed at 400 cm of the downstream from the target center to measure the charged particles in the forward direction. In order to veto the background beam particles such as π^-, K^- and $\bar{p}$, an Aerogel Cherenkov counter is placed in front of the graphite target. Finally, to suppress the faked high momentum $\pi^{\pm}$ events from combinatorial background, a gas Cherenkov counter is set at the exit of the KURAMA magnet to actively select the $P_\pi \geq 1.6$ GeV/c ($\beta_\pi \geq 0.996$) of the outgoing charged particles.

To estimate the acceptance and resolution of the experimental setup, we implemented the complete configuration in the GEANT4 simulation package and performed realistic event reconstructions using the simulated detector signals. To gain further insights into the real experimental challenges, we employed the GiBUU calculation as an event generator. This provided us with an understanding of the effects of high multiplicity and neutral particles, such as π^0.

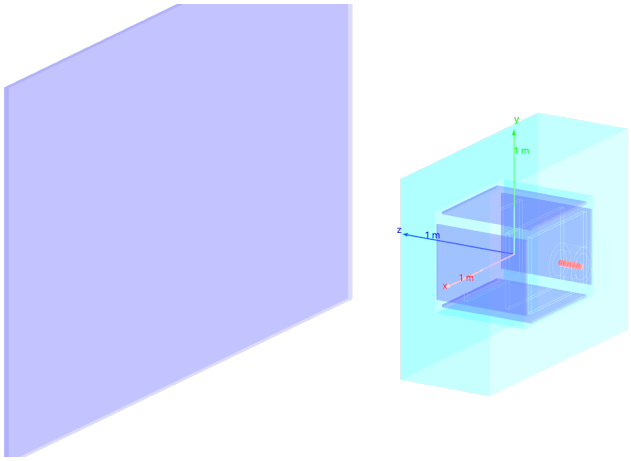

Figure 11: Schematic experimental setup. A set of thin graphite targets (10 cm total thickness) is used to fully react with the $\bar{d}$ beam particle; drift chambers are used to track the charged particles from the annihilation reaction both upstream and downstream; a barrel scintillation fiber tracker surrounds the target to catch reaction products in the central angular region; a forward TOF wall is placed downstream, at 4 m from the target center to measure the charged particles in the forward direction.

3.3 Performance estimation

According to GiBUU calculations, with the proposed 1×10^6 $\bar{d}$ particles interacting with our 10 cm thick graphite target we can expect approximately 1.3×10^5 coherent annihilation and 4.0×10^5 partial

annihilation reaction events. Using these calculated events as input for the GEANT4 simulation of the proposed setup, we can estimate the acceptance and resolution of the experiment.

Particle identification (PID) with our proposed setup, accounting for detector resolution and acceptance, is illustrated in Fig. 12. PID relies on the momentum and mass squared of the particles. As shown in Fig. 12, $\pi/K/p/d$ momentum and mass squared are distinctly separated from each other, enabling precise identification of $\pi^{\pm}$ particles. After selecting reconstructed $\pi^{\pm}$ based on mass, we find that the final acceptance for charged π with momentum $\geq$ 1.6 GeV/c is approximately 30%. As a result, we expect to detect 500 $\sim$ 1000 $\pi^{\pm}$ with momentum $\geq$ 1.6 GeV/c from both Cascade Correlated Annihilation and One-Step Simultaneous Annihilation combined, which is one order of magnitude more than the Fermi motion contribution. This estimation is based on the GiBUU calculation, which gives the Cascade Correlated Annihilation events and also our phase space based estimation for One-Step Simultaneous Annihilation by assuming a 20% of SRC states for both $\bar{d}$ and ^{12}C nucleus. [5]

Track multiplicity and decomposition are depicted in Fig. 13. A distance of the closest approach (DCA) based vertex cut has been applied to the track reconstruction to suppress combinatorial background due to large multiplicity. Only the combination that gives the smallest summed DCA is considered as the current reconstructed vertex.

The multiplicity distribution with one $\bar{p}$ detected by the forward TOF wall is used to calibrate the charge multiplicity for part of the partial annihilation events. The complete multiplicity distribution for partial annihilation can be obtained by adding back the events where $\bar{n}$ flies out, which can be achieved by shifting the $\bar{p}$ event multiplicity by -1. These two cases are shown in Fig. 13 as red and blue dashed lines as gaussian functions, respectively. The multiplicity distribution for coherent annihilation can then by derived by adding a gaussian fit function to fit the total multiplicity distribution as given in magenta line in Fig. 13, where the cyan shows the over all fit function. The yield for both partial and coherent annihilation can be obtained by integrating the fitted functions. Our simulation demonstrates a precision better than 20% for the multiplicity decomposition and thus $\sigma_{ParAnn}/\sigma_{CohAnn}$ precision.

Another uncertainty for σ_{ParAnn} and σ_{CohAnn} measurement arises from misidentification of successive partial annihilation events within the vertex resolution as coherent annihilation. To suppress this effect, we propose using a sliced thin graphite target with 1 cm thickness, as successive partial annihilation within the same target slice can be suppressed to less than 5%. Considering other sources of ambiguity such as bias and efficiency in identifying annihilation events, we anticipate achieving an overall experimental precision of approximately 20% based on our simulations.

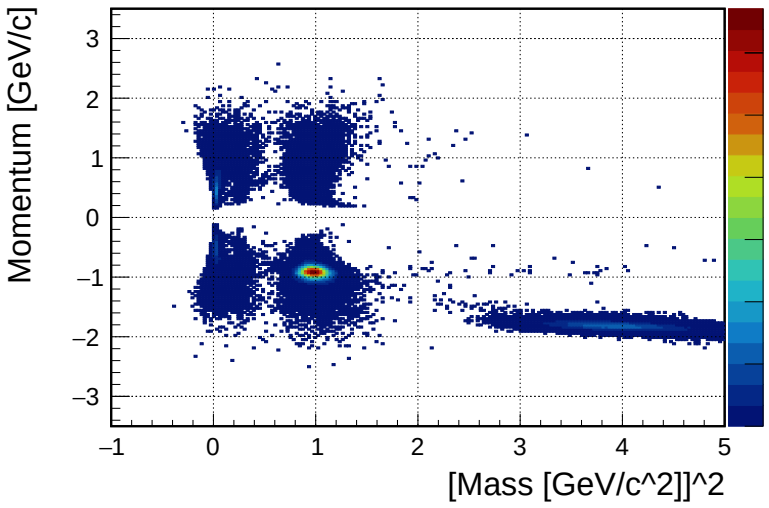

Figure 12: Particle identification for reconstructed events. $\pi/K/p/d$ can be clearly separated.

[5] This assumption gives 4% of One-Step Simultaneous Annihilation among all coherent annihilation events.

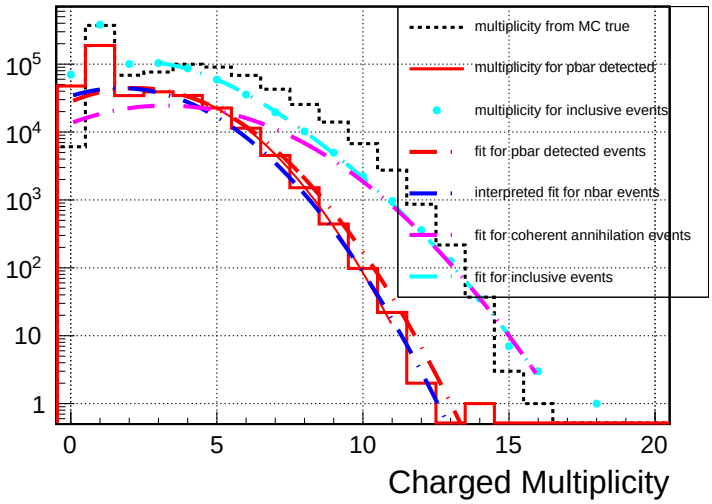

Figure 13: Track multiplicity and decomposition. Points in black represent the charge multiplicity from MC true information for reference. $\bar{p}$ events detected by the forward TOF are used to calibrate the multiplicity distribution for partial annihilation events as shown in red dashed lines. $\bar{n}$ events are assumed to have the same multiplicity distribution as $\bar{p}$ events but shift by -1 due to the charge difference between $\bar{p}$ and $\bar{n}$. The total multiplicity is then fitted by adding partial annihilation and coherent annihilation as shown in cyan line, with the magenta line representing the contribution from coherent annihilation as a gaussian function.

4 Summary

We propose to investigate the antideuteron physics at J-PARC K1.8 beam line as a first step towards study antimatter composed of multiple antinucleons. The main topics to be addressed are the $\bar{d}-$nucleus optical potential and the multiple $\bar{N}-N$ annihilation mechanism. The effectiveness of the proposed method is demonstrated through calculations using the GiBUU package. An optimized experimental setup is proposed. The acceptance and resolution of the experimental setup are estimated using GEANT4 simulations, and the performance of the proposed method is evaluated.

The proposed experiment will provide valuable insights into the $\bar{d}-$nucleus optical potential and the multiple $\bar{N}-N$ annihilation mechanism. The results will contribute to our understanding of antimatter-matter interactions and provide a foundation for future studies of antinuclei with multiple antinucleons.

References

[1] E. Widmann *et al.*, Hyperfine Interact. 240 (2019) 5

[2] The STAR Collaboration, Nature Physics 16 (2020) 409

[3] Angles & Demons (2009) directed by R. Howard, Columbia Pictures

[4] Th. Walcher *et al.*, Ann. Rev. Nucl. Part. Sci. 38 (1988) 67

[5] F. Binon *et al.*, Phys. Lett. B 31 (1970) 230

[6] S. P. Denisov *et al.*, Nucl. Phys. B 31 (1971) 253

[7] S. Acharya *et al.*, Phys. Rev. Lett. 125 (2020) 162001

[8] O. Chamberlain *et al.* Phys. Rev. Lett. 100 (1955) 947

[9] A. B. Larionov *et al.*, Phys. Rev. C 80 (2009) 021601

[10] E. Friedman *et al.*, Nucl. Phys. A 761 (2005) 283

[11] C. J. Batty, Rep. Prog. Phys. 52 (1989) 1165

[12] D. Garreta, *et al.*, Phys. Lett. 149B (1984) 64

[13] R. Subedi, *et al.*, Science 320 (2008) 1476

[14] M. Ukai, *et al.*, arXiv:2312.11821

[15] F. Iazzi, Nucl. Phys. A 655 (1999) 371c

[16] J. R. Sanford and C. L Wang, BNL report 11479 (1967)

[17] C. Van Der Leun and C. Alderliesten, Nucl. Phys. A 380 (1982) 261

[18] E. H. Auerbach, *et al.*, Phys. Rev. Lett. 46 (1981) 702

[19] V. Flaminio *et al.*, CERN-HERA 84-01 (1984)

[20] I. Tanihata, *et al.*, Phys. Rev. Lett. 55 (1985) 2676

[21] R. B. Wiringa, V. G. J. Stoks, and R. Schiavilla, Phys. Rev. C 51 (1995) 38

[22] A. B. Larionov *et al.*, Phys. Rev. C 78 (2008) 014604

[23] O. Buss *et al.*, Phys. Rep. 512, (2012) 1